Proceedings of the ASME 2018 Dynamic Systems and Control Conference
DSCC 2018
September 30-October 3, 2018, Atlanta, USA

DSCC2018-9094

APPLICATION OF MIXED H_2/H_∞ DATA DRIVEN CONTROL DESIGN TO DUAL STAGE HARD DISK DRIVES

Omid Bagherieh
Dept. of Mech. Engineering
University of California
Berkeley, California 94720
Email: omidba2@berkeley.edu

Prateek Shah*
Dept. of Mech. Engineering
University of California
Berkeley, California 94720
prateekshah@berkeley.edu

Roberto Horowitz
Dept. of Mech. Engineering
University of California
Berkeley, California 94720
horowitz@me.berkeley.edu

ABSTRACT

A data driven control design approach in the frequency domain is used to design track following feedback controllers for dual-stage hard disk drives using multiple data measurements. The advantage of the data driven approach over model based approach is that, in the former approach the controllers are directly designed from frequency responses of the plant, hence avoiding any model mismatch. The feedback controller is considered to have a Sensitivity Decoupling Structure. The data driven approach utilizes H_∞ and H_2 norms as the control objectives. The H_∞ norm is used to shape the closed loop transfer functions and ensure closed loop stability. The H_2 norm is used to constrain and/or minimize the variance of the relevant signals in time domain. The control objectives are posed as a locally convex optimization problem. Two design strategies for the dual-stage hard disk drive are presented.

INTRODUCTION

The spread of the Internet and the ever increasing demand for storage capacity is requiring more efficient storage options. Hard disk drives (HDDs) and the Solid State Drives (SSDs) are the widely used data storage options. HDDs are primarily used at data centers, while SSDs are primarily used in personal computers [1].

To increase the density of tracks in a HDD it is necessary to have a precise track following feedback controller. The control objective of a feedback controller is to stabilize the actuators while achieving certain performance levels, for example, minimizing the track positioning error of the read/write head in a HDD [2]. The most common HDD, the dual-stage HDD uses two actuators attached in series to position the read/write head onto the track [3–6].

The controllers for the dual stage HDD can be designed either by using plant models for the actuators or by using the frequency response data measurements of these actuators. The method based on the plant models is traditionally known as the model based design approach [7, 8] whereas, the method utilizing the frequency response data sets is known as the data driven control design approach [9–11]. One of the most important advantages of the data driven control methodology presented in this paper is that it solves the mixed H_2/H_∞ synthesis problem and the controller is synthesized directed based on the frequency response measurements of the actuators. Moreover, in the cases when multiple frequency response data is used and are sufficient to represent plant variations and the resonant modes of the system, the stability margins and performance specifications achieved during the design stage are assured to be met during implementation on the actual dual-stage HDD [12, 13]. There are several reasons for having multiple frequency response measurements of a given actuator. The first is to account for slow time varying variations in the actuator dynamics, which for example can be due to environmental variations such as temperature. The second is that dual-stage actuators in HDDs that have multiple disk platters also have multiple second-stage actuators and the dynamics of the second-stage actuator may vary significantly depending on the disk (inner versus outer) that the actuator

*Address all correspondence to this author.

is located on. Since data is stored along multiple platters the dynamics of the dual stage HDD can change depending on the disk platter in which the data is being stored on. Finally, there often exist significant dynamic variations among different units of a HDD product line and the same controller may be used among all units of the product line.

The data driven control design methodology in the frequency domain transforms the H_2 norm and H_∞ norm of the closed loop transfer functions into an optimization problem where H_2 norm and H_∞ norm of the closed loop transfer functions are posed as an objective function and/or constraints. The data driven H_∞ control problem for single-input single-output (SISO) systems was addressed in [11], where the H_∞ norm condition was transformed into a necessary and sufficient convex condition. This H_∞ control design methodology is extended to multi-input single- output (MISO) controlled plants in [13], which is the most frequently encountered situation in the design of track -following controllers for dual-stage actuators. A sufficient convex constraint for the H_2 norm condition for multi-input multi-output (MIMO) systems was presented in [10]. The data driven H_2 control problem for SISO systems with pre-specified control structure like Finite Impulse Response (FIR) filters was given in [12]. The data driven H_2 control for MIMO systems with a general control structure was presented in [10].

The H_∞ norm and H_2 norm control conditions can be simultaneously considered as a mixed H_2/H_∞ norm control problem [10,13,14]. Also, [13] presents an approach which considers multiple data measurements simultaneously. This problem formulation is used to design a feedback controller for dual-stage HDDs. The dual stage HDD has two actuators, voice coil motor (VCM) and the milli-actuator (MA), to position the read/write head onto the track It accepts two control inputs, one for each of the two actuators and has only one measurement output. That is, the dual-stage HDD is a MISO system. Therefore, the controller for this system will be a single-input multi output (SIMO) controller. Conventionally, the dual-stage HDD is decoupled into two SISO systems using sensitivity decoupling [3–7]. Hence, the controllers for the two SISO systems can be obtained sequentially by considering two mixed H_2/H_∞ optimization problems. This strategy is the *sequential SISO design strategy* [13]. Another viable strategy is to directly design a single-input double-output controller for the dual-stage HDD. This strategy solves the mixed H_2/H_∞ design problem developed for MISO systems. In this strategy, the SIMO control block will be obtained directly in a single step. This strategy is called the *SIMO design strategy* [13]. The main advantage of the SIMO design strategy is that both the controllers are designed in one step rather than having one controller fixed while the second controller is being designed.

Summarizing, the problem statement of the mixed H_2/H_∞ data driven control design methodology for a dual-stage HDD is to design a feedback controller with a SIMO structure based on the multiple frequency response data measurements of the two actuators of the dual stage HDD. The measurement noise data and the track run-out data are also available to the designer during the design phase.

PRELIMINARIES

In this section, the stable factorizations for the frequency response measurement of the plant and the controller transfer function followed by the feedback structure used to design the controller are discussed. We consider the control of discrete-time multi-input, single-output (MISO) rational causal transfer functions plants $G(z) \in \mathbb{R}_p^{1\times n}$. However, we will only use their frequency response data $G(\omega)$ for $\omega \in \Omega = \left\{\omega | -\frac{\pi}{T_s} \leq \omega \leq \frac{\pi}{T_s}\right\}$ with T_s being the sample time, except for the finite number of frequencies that correspond to the poles of G. Our goal is to design a discrete time single-input, multi-output (SIMO) controller $K(z) \in \mathbb{R}_p^{n\times 1}$, which can be realized by a discrete-time rational causal transfer function. The frequency response of the controller can be generated $K(e^{j\omega})$. We will often drop the arguments of the plant and controller transfer functions to simplify notation and we may include dimensional subscripts, e.g. $G_{1\times n}(\omega)$ for clarity.

Plant and Controller Factorization

The stable factorizations from [15] are used for the plant, $G_{1\times n}(\omega)$, and the controller, $K_{n\times 1}(z)$ from Fig. 1, in the data driven control design as given below

$$G_{1\times n}(\omega) = \tilde{M}_{1\times 1}^{-1}(\omega)\tilde{N}_{1\times n}(\omega) \tag{1}$$

$$K_{n\times 1}(z) = X_{n\times 1}(z)Y_{1\times 1}^{-1}(z) \tag{2}$$

where $\tilde{M}_{1\times 1} \in \mathbb{RH}_\infty^{1\times 1}$, $\tilde{N}_{1\times n} \in \mathbb{RH}_\infty^{1\times n}$, $X_{n\times 1} \in \mathbb{RH}_\infty^{n\times 1}$ and $Y_{1\times 1} \in \mathbb{RH}_\infty^{1\times 1}$ are all asymptotically stable rational proper transfer functions. The factorizations are true for frequency domain as well as the z domain. The stable factorizations can be converted to frequency domain from the z domain simply by substituting z by $e^{j\omega}$. The stable factorizations for the plant $G_{1\times n}(\omega)$ need to be obtained carefully, since only frequency domain data is available. It is straight forward to obtain the stable factorizations when $G(\omega)$ is stable. The factorizations can be obtained even when $G(\omega)$ is known to be a product of some known marginally stable poles and a stable $G^0(\omega)$ or for an unstable plants, as described in [13]. In this paper we will factorize the controller $K(z)$ using finite impulse responses filters (FIRs), with all poles at the origin.

$$X(z) = X_p z^p + X_{p-1}z^{p-1} + \cdots + X_o \tag{3}$$
$$Y(z) = z^p + Y_{p-1}z^{p-1} + \cdots + Y_o$$

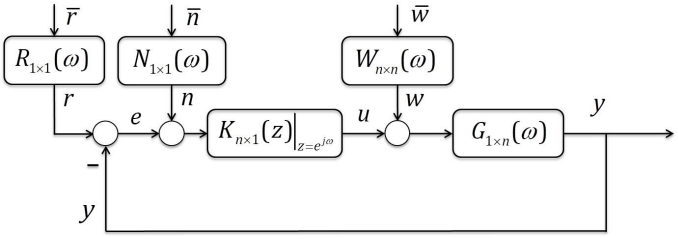

FIGURE 1. Block Diagram of a data driven control design setup

where p is the controller order and the controller parameters $\{Y_{p-1},\cdots,Y_o\} \in \mathscr{R}$ and $\{X_p,\cdots,X_o\} \in \mathscr{R}^{n\times1}$ are to be determined.

Feedback Structure

Fig. 1 shows the basic feedback structure used to design the controller $K(z)$. The lower case letters represent discrete time sequences (also loosely referred to as signals). We will now obtain expressions for the closed loop transfer functions, which will be denoted by an upper case letter and a subscript that represents its input to output causality, in terms of the controller and plant factorizations. For example, $E_{r\to e}$ denotes the closed loop transfer function from the track runnout input r to the tracking error output e. r, n, and w are the track run-out, measurement noise and windage respectively. As the plant, $G(\omega)$ in Fig. 1, is in the form of frequency response data, all the closed loop transfer functions will be obtained in the frequency domain. The closed loop transfer functions from the external signals (r, n and w) to the tracking error e, the control input signal u and the output y are

$$\begin{bmatrix} E_{r\to e} & E_{n\to e} & E_{w\to e} \\ U_{r\to u} & U_{n\to u} & U_{w\to u} \\ Y_{r\to y} & Y_{n\to y} & Y_{w\to y} \end{bmatrix} = \frac{1}{\tilde{N}X+\tilde{M}Y} \begin{bmatrix} \tilde{M}Y & -\tilde{M}Y & -\tilde{N}Y \\ \tilde{M}X & \tilde{M}X & -X\tilde{N} \\ \tilde{N}X & \tilde{N}X & \tilde{N}Y \end{bmatrix}. \quad (4)$$

For notational compactness, we have dropped the frequency domain arguments.

DATA DRIVEN CONTROL DESIGN

This section summarizes the use of H_∞ and H_2 norm constraints on closed loop transfer functions, in the data-driven setup. In data-driven control design, these norms are used to design constraints in the frequency domain to achieve desired stability and performance levels. Consider that we have l frequency response measurements available for the plant. Let $G_i(\omega) = \tilde{M}_i^{-1}(\omega)\tilde{N}_i(\omega)$ represents the i^{th} frequency response measurement, and its respective factorizations.

H_∞ norm

For a stable single-input single-output (SISO) system, the H_∞ norm is defined as the peak gain, the largest value of the frequency response magnitude; whereas, for a multi-input multi-output (MIMO) system, the H_∞ norm is defined as the largest singular value across the frequency range Ω.

We now consider bounding the weighted H_∞ norm of the closed loop sensitivity transfer function

$$U_{w\to u} = -X\tilde{N}(\tilde{N}X+\tilde{M}Y)^{-1} \quad (5)$$

for all plant l frequency response measurements:

$$||W_{U_{w\to u}}U_{(w\to u)i}||_\infty = \bar{\sigma}\left(W_{U_{w\to u}}(\omega)U_{(w\to u)i}(\omega)\right) < \gamma \quad (6)$$

$\forall i \in 1\ldots l$, where $\bar{\sigma}(A)$ is the maximum singular value of matrix A, $U_{(w\to u)i}(\omega)$ is the i^{th} frequency response data set of the closed loop sensitivity function $U_{w\to u}$ in Eq. (5), $W_{U_{w\to u}}(\omega)$ is a bounded weighting function and γ is a positive constant.

The H_∞ norm condition in Eq. (6) can be transformed into a convex constraint in the frequency domain as developed for SISO systems in [11] and extended for MISO plants in [13]. The theorem from [13] is stated below.

Theorem 1: *Assume that i^{th} frequency response data measurement of the plant is given $G_i(\omega)$ over the frequency region Ω, and is factorized according to Eq. (1). Given a positive scalar γ, the following two statements are equivalent.*

I Controller $K(z)$ stabilizes the plant $G_i(\omega)$ and

$$||W_{U_{w\to u}}U_{(w\to u)i}||_\infty < \gamma \quad (7)$$

II There exists controller stable factorizations $X_{n\times1}(z)|_{z=e^{j\omega}}$, $Y_{1\times1}(z)|_{z=e^{j\omega}}$ according to Eq. (2), such that the following convex inequality holds,

$$\gamma^{-1}\bar{\sigma}(W_{U_{w\to u}}(\omega)X(e^{j\omega})\tilde{N}_i(\omega)) < Re(\tilde{N}_i(\omega)X(e^{j\omega})+\tilde{M}_i(\omega)Y(e^{j\omega})) \quad (8)$$

$Re(r)$ represents the real part of complex number r.

Notice that the constraint (8) is convex in the controller parameters $\{X_p,\cdots,X_o\} \in \mathscr{R}^n$ and $\{Y_{p-1},\cdots,Y_o\} \in \mathscr{R}$ in Eq. (3). In practice the convex constraint (8) is evaluated for a finite set of frequencies

$$\Omega_N = \{\omega_1,\cdots,\omega_N\},\ \omega_i \in \Omega = (-\frac{\pi}{T_s},\frac{\pi}{T_s}) \quad (9)$$

Similar convex constraints can be obtained for the weighted H_∞ norms of the other components of the closed loop sensitivity transfer function in Eq. (4). The wighting function $W_{U_{w\to u}}$ and others must be selected by the designer in order to shape the desired closed loop sensitivity transfer functions. Further details are presented in the application to dual-stage HDDs section.

H_2 norm

According to the Parseval's Theorem, the H_2 norm of a transfer function is equal to the square root of the variance of the output of the transfer function, in time domain. Therefore, H_2 norm can be used to constrain the variance of the signals in time domain. Throughout this paper we assume that the exogeneous random variables r, w and n are zero-mean independent unit variance white noises. Therefore, the variance of the tracking error $e = r - y$ is given by

$$||e||_2^2 = ||E_{r\to e}R||_2^2 + ||E_{w\to e}W||_2^2 + ||E_{n\to e}N||_2^2 \qquad (10)$$

where, R, W and N are open loop transfer functions used to filter the external signals $\bar{r}$, $\bar{w}$ and $\bar{n}$ in Fig. 1. In the data driven design methodology presented in this paper, we will both constrain the H_2 norm of some signals for all l frequency reponses of the plant, e.g.

$$||u_i||_2^2 \le \beta_u \Rightarrow ||U_{(r\to u),i}R||_2^2 + ||U_{(w\to u),i}W||_2^2 + ||U_{(n\to u),i}N||_2^2 \le \beta_u$$

for $i = 1, \cdots l$, or minimize the average variance of a signal across l data measurements, e.g.

$$\frac{1}{l}\sum_{i=1}^{l}||e_i||_2^2 = \frac{1}{l}\sum_{i=1}^{l}\left[||E_{(r\to e),i}R||_2^2 + ||E_{(w\to e),i}W||_2^2 + ||E_{(n\to e),i}N||_2^2\right] \qquad (11)$$

where for example, the H_2 norm $||E_{(r\to e),i}R||_2^2$ for the i^{th} plant frequency response data is given by

$$||E_{(r\to e),i}R||_2^2 = \frac{1}{2\pi}\int_\Omega tr\left(R^*(\omega)E^*_{(r\to e),i}(\omega)E_{(r\to e),i}(\omega)R(\omega)\right)d\omega$$

and the frequency weights $R(\omega)$, $W(\omega)$ and $N(\omega)$ characterize the exogenous random disturbance inputs and, for example, $E^*_{(r\to e),i}(\omega)$ is the closed loop sensitivity frequency response based on the i^{th} plant model frequency responde data.

The following result from [10] is used to determine an upper bound to H_2 norms.

Theorem 2: *Given l factorized frequency responses data, where the i^{th} plant measurement $G_i(\omega) = \tilde{M}_i^{-1}(\omega)\tilde{N}_i(\omega)$ is given over the frequency region Ω, and an initial factorized stabilizing controller $K_{k-1}(z) = X_{k-1}(z)Y_{k-1}(z)^{-1}$, an upper bound of the average variance tracking error variance defined in (12) can be computed as follows*

$$\min_{X_k(z),Y(z)} \frac{1}{l}\sum_{i=1}^{l}||e_i||_2^2 \le \qquad (12)$$

$$\min_{X_k(z),Y_k(z)} \frac{1}{2\pi l}\sum_{i=1}^{l}\int_\Omega \left[tr(\Gamma^i_{E_{r\to e}}(\omega)) + tr(\Gamma^i_{E_{n\to e}}(\omega)) + tr(\Gamma^i_{E_{w\to e}}(\omega))\right]d\omega$$

$\forall i \in 1, ..., l$, and $\forall \omega \in \Omega$:

$$\begin{bmatrix}\Gamma^i_{E_{r\to e}} & Y_k\tilde{M}_iR \\ R^*\tilde{M}_i^*Y_k^* & P^*_{k,i}P_{k-1,i} + P^*_{k-1,i}P_{k,i} - P^*_{k-1,i}P_{k-1,i}\end{bmatrix}(\omega) \succ 0 \qquad (13)$$

$$\begin{bmatrix}\Gamma^i_{E_{n\to e}} & Y_k\tilde{M}_iN \\ N^*\tilde{M}_i^*Y_k^* & P^*_{k,i}P_{k-1,i} + P^*_{k-1,i}P_{k,i} - P^*_{k-1,i}P_{k-1,i}\end{bmatrix}(\omega) \succ 0 \qquad (14)$$

$$\begin{bmatrix}\Gamma^i_{E_{w\to e}} & \tilde{N}_iY_kW \\ W^*Y_k^*\tilde{N}_i^* & P^*_{k,i}P_{k-1,i} + P^*_{k-1,i}P_{k,i} - P^*_{k-1,i}P_{k-1,i}\end{bmatrix}(\omega) \succ 0 \qquad (15)$$

$$P_{k,i} = \tilde{N}_iX_k + \tilde{M}_iY_k\,, \qquad P_{k-1,i} = \tilde{N}_iX_{k-1} + \tilde{M}_iY_{k-1} \qquad (16)$$

Eqs. (13)-(15) are Linear Matrix Inequalities (LMIs) and hence convex constraints in in the controller $K_k(z)$ parameters $\{X_{p,k}, \cdots, X_{o,k}\} \in \mathscr{R}^n$ and $\{Y_{p-1,k}, \cdots, Y_{o,k}\} \in \mathscr{R}$ in Eq. (3). But, the equations are local and iterative as they are dependent of the controller $K_{k-1}(z)$ from the previous iteration. Theorem 2 transforms the H_2 norm condition to a sufficient convex constraint. The integral in (12) is normally approximated by quadratures and the LMIs are evaluated for a finite set of frequencies $\Omega_N = \{\omega_1, \cdots \omega_N\}$. Hence the matrix functions $\Gamma^i_{E_{r\to e}}$, $\Gamma^i_{E_{n\to e}}$, and $\Gamma^i_{E_{w\to e}}$ in (12)-(15) each become a collection of matrices evaluated at each frequency, e.g. $\Gamma^i_{E_{r\to e}}(\omega) = \{\Gamma^i_{E_{r\to e}}(\omega_1)), \cdots, \Gamma^i_{E_{r\to e}}(\omega_N))\}$.

Theorem 2 can be used to obtain a feedback controller while minimizing or constraining an H_2 norm condition. But, this theorem does not guarantee closed loop stability. Under the conditions that the order and poles at the unit circle of the controllers $k_k(z)$ and $k_{k-}(z)$ remain the same with each iteration, a controller initialization approach and the use of an additional iterative constraint $Y_k^*Y_{k-1} + Y_{k-1}^*Y_k - Y_{k-1}^*Y_{k-1} > 0$. is proposed in [10] to guarantee that the controller $K_k(z)$ is stabilizing at each iteration. In this paper however, we will perform mixed H_2/H_∞ norm optimizations, as described in the next section. Since the satisfaction of the H_∞ convex constraint (8) in Theorem 1 guarantees that the synthesized controller $K_k(z)$ is stabilizing at each iteration, it is not necessary to impose additional constraints to (12)-(15) in theorem 2.

Mixed H_2/H_∞ Norm Optimization

The mixed H_2/H_∞ norm problem is characterized by the minimization of the H_2 norm of a closed loop transfer function and the application of H_2 and H_∞ norms constraints.

Using Theorem 1 and Theorem 2 for the data driven setup, the mixed H_2/H_∞ problem can be transformed into a locally convex optimization problem which has an iterative solution [13]. Fig. 5.2 in [13] gives the flow chart of the iterative optimization problem to be implemented. Mixed H_2/H_∞ norm optimization problem is used to obtain feedback controllers for dual-stage HDDs in the data-driven setup.The problem formulation is explained in the next section.

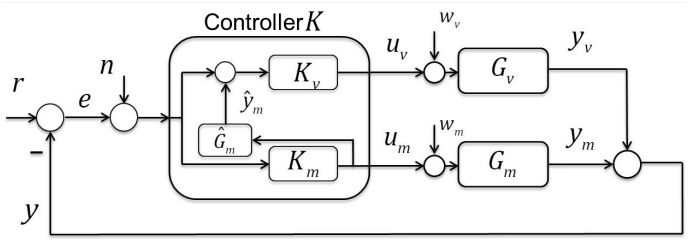

FIGURE 2. Sensitivity Decoupling Structure

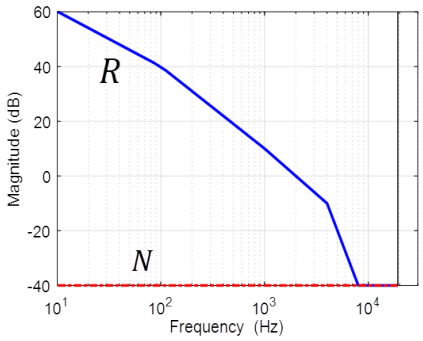

FIGURE 3. Measurement Noise and Run-out. Following a conventional industry practice, w_v and w_m are assumed to be zero and their effects are incorporated in the definitions of R and N.

APPLICATION TO DUAL STAGE HDDs

In a dual stage Hard Disk drive, the Voice Coil Motor (VCM) and the Milli- Actuator (MA) are the two actuators used to achieve track following and track seeking control. The block diagram for a dual stage hard disk drive is shown in Fig. 2. G_v and G_m are VCM and MA respectively. u_v and u_m are their inputs and y_v and y_m are their corresponding outputs. There are three sources of external noise and disturbance in the form of windage (w_v and w_m) and measurement noise (n). Track run-out (r) acts as the reference for the feedback control.

Our objective is to design the controller K to achieve track following based on the frequency response measurements of actuators G_v and G_m for the known spectrum of track run-out r and measurement noise n, as shown in Fig. 3. Multiple data measurements of G_v and G_m are used to design a common controller for all the $G_v - G_m$ pairs.We assume the windage w_v and w_m are lumped into the run-out r and measurement noise n.

The control structure used for the dual stage HDD is the sensitivity decoupling structure as illustrated in Fig. 2. Sensitivity decoupling states that the sensitivity of the entire closed loop is approximately equal to the sensitivity of the VCM loop times the sensitivity of the MA loop [3–5].

$$S = \frac{1}{1+K_mG_m+K_vG_v(1+K_mG_m)} = S_vS_m \tag{17}$$
$$S_v = \frac{1}{1+K_vG_v};\ S_m = \frac{1}{1+K_m\bar{G}_m} \approx \frac{1}{1+K_mG_m}$$
$$\bar{G}_m = G_m + \frac{K_vG_v(\hat{G}_m - G_m)}{1+K_vG_v}$$

The advantage of sensitivity decoupling is that the closed loop stability of the single stage loops as well as the dual stage loop can be ensured with appropriate constraints. In case the milli-actuator fails, the signals u_m and $\hat{y}_m$ in Fig. 2 can be cut off and the HDD will perform as a single-stage HDD.

Our objective is to obtain a stabilizing controller for the dual-stage HDD whose frequency response data measurements, spectrum of the track run-out and measurement noise are available to the designer. The controller designed should stabilize the HDD and meet certain robust control objectives which will be mentioned in the next section. Two control strategies will be illustrated to design a controller with the sensitivity decoupling structure. They are: the sequential SISO design strategy and the SIMO design strategy.

Sequential SISO Design Strategy

In this strategy the SISO controller K_v is first designed for the single-stage VCM (by cutting the the signals u_m and $\hat{y}_m$ in Fig. 2). In the second step, for the fixed VCM controller K_v designed during the first step, the SISO controller K_m is designed for the dual-stage loop again using SISO performance and constraints. The first step of this strategy ensures that the HDD remains stable in case the MA fails.

The control objectives are considered in terms of constraints on the H_∞ and H_2 norms of the closed loop transfer functions of the dual-stage HDD in frequency domain. The H_∞ norm will be used to shape the closed loop transfer functions whereas, the H_2 norms of the closed loop transfer functions will be used to constrain and/or minimize the variance of corresponding signals in the time domain.

The H_∞ norm of the closed loop transfer functions will be constrained for both, the single stage VCM loop and the dual stage loop. The following H_∞ norm constraints are imposed in the first step, for the single stage HDD. The closed loop transfer functions used in this section are according to Eq.(4).

$$\begin{aligned}&\forall i \in 1,\dots l:\\ &\quad ||W_{E^s_{r\to e}}E^s_{(r\to e),i}||_\infty < 1,\ ||W_{U^s_{r\to u_v}}U^s_{(r\to u_v),i}||_\infty < 1,\\ &\quad ||W_{E^s_{w_v\to e}}E^s_{(w_v\to e),i}||_\infty < 1,\ ||W_{U^s_{w_v\to u_v}}U^s_{(w_v\to u_v),i}||_\infty < 1.\end{aligned} \tag{18}$$

where $W_H(\omega)$ is a weighting function in the frequency domain for the closed loop transfer function H. The superscript H^s denotes the single-stage HDD with the VCM as the actuator. For

example, $E^s_{(r\to e),i} = S_{vi}$, where S_{vi} is VCM's closed loop sensitivity transfer function, as defined in Eq. (17), using the i^{th} VCM frequency response data, $G_{v,i}(\omega)$.

The H_∞ norm constraints for the dual stage HDD are imposed in a similar manner.

$$\begin{aligned}&\forall i \in 1,\dots l:\\ &||W_{E_{r\to e}} E_{(r\to e),i}||_\infty < 1,\ ||W_{U_{r\to u_v}} U_{(r\to u_v)),i}||_\infty < 1,\\ &||W_{E_{w\to e}} E_{(w\to e),i}||_\infty < 1,\ ||W_{U_{w\to u_v}} U_{(w\to u_v),i}||_\infty < 1. \quad (19)\end{aligned}$$

$$\text{where} \qquad u = \begin{bmatrix} u_v & u_m \end{bmatrix}^T, w = \begin{bmatrix} w_v & w_m \end{bmatrix}^T. \quad (20)$$

The primary objective in track following control is to minimize the position tracking error, that is the variance of the tracking position error signal (PES), e, given by $||e||_2^2$. In this paper we will synthesize controllers that minimize the average variance of the PES of the dual-stage loop for a l sets of plant frequency response data, as defined in Eq. (12), under the H_∞ constraints given in Eqs. (18) and (19), and by imposing additional H_2 constraints, as detailed subsequently.

In the case of the sequential SISO design technique, the VCM compensator $K_v = X_v Y_v^{-1}$ is first designed to minimize the average variance of the PES under SISO VCM closed loop.

$$\frac{1}{l}\sum_{i=1}^{l} ||e_i^s||_2^2 = \sum_{i=1}^{l} (||E^s_{(r\to e),i} R||_2^2 + ||E^s_{(n\to e),i} N||_2^2 + ||E^s_{(w_v\to e),i} W_v||_2^2) \quad (21)$$

Subsequently, the MA actuator, $K_m = X_m Y_m^{-1}$, is designed.

It is important to consider the actuator limitations in the form of limits on stroke and input signals. It is advisable to constrain the average input variance to the VCM, both when the VCM is functioning as a single stage actuator in a SISO feedback loop

$$\begin{aligned}\frac{1}{l}\sum_{i=1}^{l} ||u^s_{vi}||_2^2 = \sum_{i=1}^{l} (&||U^s_{(r\to u_v),i} R||_2^2 + ||U^s_{(n\to u_v),i} N||_2^2 \\ &+ ||U^s_{(w_v\to u_v),i} W_v||_2^2) < \eta_{u_v^s}, \quad (22)\end{aligned}$$

or as the corse actuator in a dual stage servo system under the sensitivity decoupling structure

$$\begin{aligned}\frac{1}{l}\sum_{i=1}^{l} ||u_{vi}||_2^2 = \sum_{i=1}^{l} (&||U_{(r\to u_v),i} R||_2^2 + ||U_{(n\to u_v),i} N||_2^2 \\ &+ ||U_{(w_v\to u_v),i} W_v||_2^2) + ||U_{(w_m\to u_v),i} W_m||_2^2) < \eta_{u_v}. \quad (23)\end{aligned}$$

In the case of the PZT microactuator (MA), it is important to constrain the average variance of the microactuator stroke to minimize the occurrence of it being saturated.

$$\begin{aligned}\frac{1}{l}\sum_{i=1}^{l} ||y_{mi}||_2^2 = \sum_{i=1}^{l} (&||Y_{(r\to y_m),i} R||_2^2 + ||Y_{(n\to y_m),i} N||_2^2 \\ &+ ||Y_{(w_v\to y_m),i} W_v||_2^2) + ||Y_{(w_m\to y_m),i} W_m||_2^2) < \eta_{y_m}. \quad (24)\end{aligned}$$

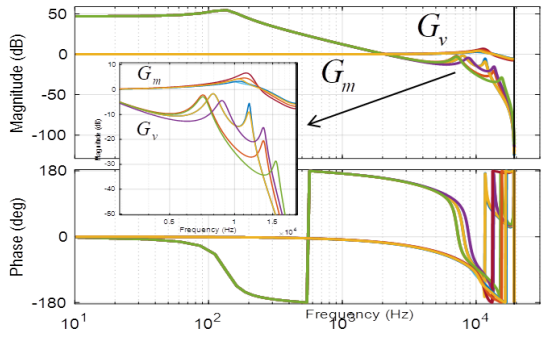

FIGURE 4. Frequency Response measurements of a dual-stage HDD. Five measurements of each actuators are used in the design. G_v and G_m represent VCM and MA actuators respectively. The actuator output units for both the VCM and MA is in '10 nm'.

Now, putting the objective functions and the constraints together, in the sequential SISO strategy, the controller K_v is first designed based on the single-stage VCM feedback loop. The corresponding locally convex optimization problem will be:

$$\begin{aligned}\min_{K_v} \quad & \frac{1}{l}\sum_{i=1}^{l} ||e_i^s||_2^2 \quad \text{defined as in Eq. (21)}\\ \text{subject to} \quad & \text{Eq. (18)} \quad H_\infty \text{ constraint}\\ & \text{Eq. (22)} \quad H_2 \text{ constraint}\end{aligned}$$

After, K_v is synthesized, the MA controller K_m is designed, via the following locally convex optimization problem

$$\begin{aligned}\min_{K_m} \quad & \frac{1}{l}\sum_{i=1}^{l} ||e_i||_2^2 \quad \text{defined as in Eq. (11)}\\ \text{subject to} \quad & \text{Eq. (19)} \quad H_\infty \text{ constraint}\\ & \text{Eqs. (23), (24)} \quad H_2 \text{ constraints}\end{aligned}$$

SIMO Design Strategy

A dual-stage hard disk drive is a MISO system. The SIMO design strategy directly designs a controller $\bar{K}_{2\times 1}$ for both the actuators of the dual-stage HDD simultaneously. The compensators for the sensitivity decoupling structure can then be obtained as follows.

$$\bar{K}_{2\times 1} = \begin{bmatrix} \bar{K}_1 \\ \bar{K}_2 \end{bmatrix} = \begin{bmatrix} K_v(1+K_m\hat{G}_m) \\ K_m \end{bmatrix} \implies \begin{cases} K_v = \frac{\bar{K}_1}{1+\bar{K}_2\hat{G}_m} \\ K_m = \bar{K}_2 \end{cases} \quad (25)$$

In the SIMO design strategy the controller $\bar{K}$ is designed considering the stability and variance constraints for both the single-stage VCM and the dual-stage HDD, simultaneously. The convex optimization problem to be solved for the SIMO design strategy to synthesize $\bar{K} = \bar{X}\bar{Y}^{-1}$ is as shown below.

$$\min_{\bar{X},\bar{Y}} \quad \frac{1}{l}\sum_{i=1}^{l}||e_i||_2^2 \quad \text{defined as in Eq. (11)}$$
$$\text{subject to} \quad \text{Eqs. (18), (19),} \quad H_\infty \text{ constraint}$$
$$\text{Eqs. (23), (24)} \quad H_2 \text{ constraints}$$

Once $\bar{K}$ is obtained, K_v and K_m can be evaluated using Eq. (25).

Design Results

In this section, the control design settings of the data driven methodology for a dual stage HDD are presented. A comparison between the sequential SISO design strategy and the SIMO design strategy is also presented.

The data driven methodology only utilizes the frequency response measurements of the plant and does not require models for the actuators. A set of five frequency response data measurements for each actuator of the dual-stage HDD are considered for the design of the feedback controller. A higher number of data measurement can be used to describe the plant dynamics if necessary. The frequency responses shown in Fig. 4 were generated using realistic models of both the VCM and MA. The data driven design approach was also implemented on a set of actual actuator measurements obtained from our HDD industrial partners which cannot be presented due to a confidentiality agreement. The noise spectrum considered for the computation of the H_2 norm is shown in Fig. 3. R and N represent the spectrum for track run-out and measurement noise respectively. A pure delayed was used for the estimated MA model, $\hat{G}_m = z^{-1}$, in the sensitivity decoupling control structure in Fig. 2, mainly to match the MA's DC gain.

The controller for the VCM actuator includes an integrator to eliminate the steady state tracking error due to DC disturbances. On obtaining the stable factorizations for the plant and the controller, the mixed H_2/H_∞ convex optimization problem is formulated. This is a locally convex problem and has to be solved iteratively. This problem is formulated using YALMIP [16] package in MATLAB and solved by the MOSEK solver. The stopping criterion for the problem is set to 10 iterations. A formal stopping criterion can also be used by defining an ε which can be the factor of reduction obtained in the objective function with every iteration.

The MAs used in dual-stage HDDs have a limited output stroke. A smaller stroke MA is more reliable and easier to manufacture. However, decreasing the stroke of the MA also affects the performance of the servo system. The controllers for the dual stage HDD were designed using four different constraint values for the average variance of the MA output stroke in Eq. (24):

$$\eta_{y_m} = 44^2,\ 42^2,\ 40^2,\ 38^2\ nm^2. \tag{26}$$

Since the compensator for the SISO design strategy will always satisfy these four constraints, only the scenario with $\eta_{y_m} = 44^2\ nm^2$ is considered. Table 1 states the five scenarios that will be analyzed and compared.

Index	Scenario	Design Strategy	$\eta_{y_m}\ (nm^2)$	Marker type
1	$SIMO_1$	SIMO	44^2	+
2	$SIMO_2$	SIMO	42^2	×
3	$SIMO_3$	SIMO	40^2	◁
4	$SIMO_4$	SIMO	38^2	▷
5	$SISO_1$	SISO	44^2	○

TABLE 1. Scenarios considered in the analysis of the design strategies

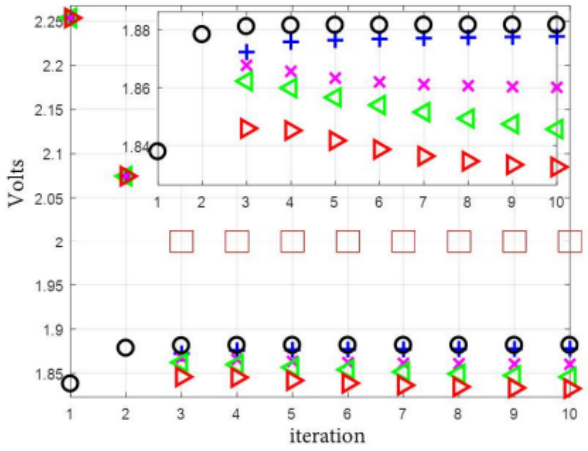

FIGURE 5. H_2 norm constraint: $\sqrt{\frac{1}{l}\sum_{i=1}^{l}||u_{vi}||_2}$. The square shows the upper bound values of the constraints used for the optimization problem. The other markers represent real values obtained, as per Table 1.

In the subsequent plots, the squares show the upper bound values of the constraints used for the optimization problem, representing either constraint imposed on the VCM control input (η_{u_v}) given by Eq. (23), or the constraint imposed on the MA output stroke (η_{y_m}), given by Eq. (24).

Dual-stage HDD

The H_2 norm constraints for the VCM input and the MA output stroke are shown in Fig. 5 and Fig. 6, respectively. In the sequential SISO design strategy the VCM is designed to be aggressive. Therefore, the variance in the input of this VCM in a dual-stage HDD will be higher as compared to the scenarios with SIMO design strategy. We can also observe that the MA with a

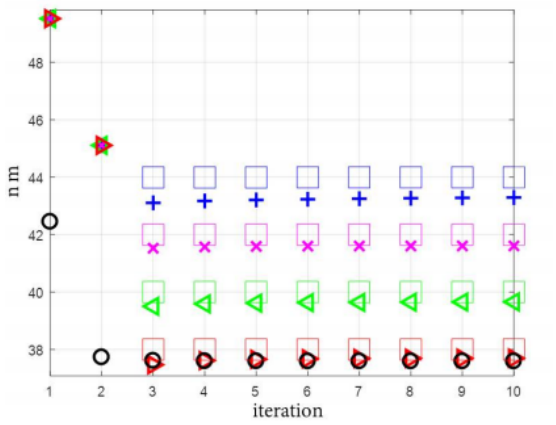

FIGURE 6. H_2 norm constraint: $\sqrt{\frac{1}{l}\sum_{i=1}^{l}||y_{mi}||_2}$. The square shows the upper bound used for the optimization problem. The other markers represent real values as per Table 1.

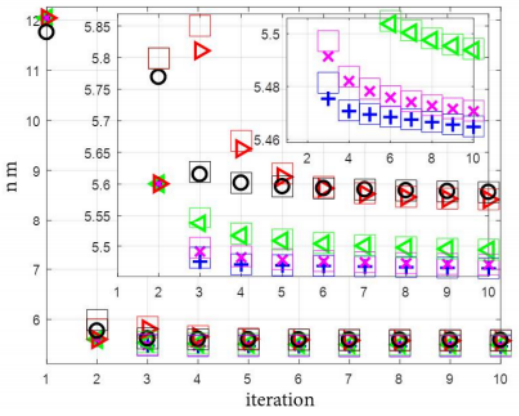

FIGURE 7. The H_2 objective $\sqrt{\frac{1}{l}\sum_{i=1}^{l}||e_i||_2}$ used for the optimization problem is plotted versus the iteration number. The square shows the upper bound used for the optimization problem. The other markers represent real values as per Table 1.

smaller output stroke gives a decreased average variance of the VCM input, in a dual-stage HDD. This can be explained by a lesser need for the VCM to rectify the out of phase MA movements, with respect to the VCM movements, due to the smaller MA stroke. Fig. 6 shows that in all the scenarios the MA satisfies the output stroke limits represented by the upper bounds.

Fig. 7 plots the square root of the average variance of the tracking error as defined in Eq. (eq:eh2ave) with respect to the iteration number for all five scenarios. The average variance of the tracking error was the objective function for the SIMO design strategy and for the second step of the sequential design strategy. In the sequential SISO design strategy, step 1 solves for the VCM compensator K_v. For the fixed K_v, step 2 minimizes the average variance in the tracking error. Therefore, the result obtained is suboptimal. This can be verified from Fig. 7, the average variance of the tracking error for the sequential SISO design strategy is larger than the average variance of the tracking error for all the scenarios of the SIMO design strategy. It can also be observed in in Fig. 7 that the average variance of the tracking error decreases with an increase in the MA output stroke.

Since the z-domain transfer functions of the actuator frequency response measurements shown in Fig. 4 are available for this example, the closed poles of the feedback system, for all the synthesized compensators of all the scenarios from Table 1, were computed and verified to yield stable feedback systems for all the plants. Table 2 gives the worst case stability margins and bandwidths for the scenarios from Table 1. [13] defines equations to obtain these worst case margins.

Scenario	$E_{r\to e}$ peak	GM	PM	ω_{GM}	ω_{PM}
	dB	dB	$degree$	Hz	Hz
$SIMO_1$	9.63	8.85	19.13	12,392	4,924
$SIMO_2$	9.62	8.85	19.14	12,393	4,922
$SIMO_3$	9.55	8.86	19.36	12,390	4,914
$SIMO_4$	9.43	8.87	19.74	12,401	4,884
$SISO_1$	9.58	8.90	19.23	12,377	4,857

TABLE 2. Worst case open Loop stability margins and bandwidths

VCM Single Stage

We now consider the event in which the MA has failed in a HDD deployed to the market. In such an event, the MA control signal u_m and the estimated MA position $\hat{y}_m$ are cut in the control structure in Fig. fig:siso and the VCM operates as a SISO feedback system. A comparison of the performance of the control systems designs in Table 1 is discussed under this scenario. The average H_2 norms of the tracking error (optimization objective) and the VCM input (constraints) for the VCM single-stage loop are shown in Fig. 8 and Fig. 9 respectively. In the sequential SISO design strategy the objective in step one is to minimize the average variance of the VCM single-stage tracking error. But, in the SIMO design strategy, the minimization of the variance of the dual-stage tracking error is performed. Therefore, the SIMO design strategy does not explicitly consider the average variance of the single-stage VCM tracking error. This is apparent in Fig. 8, the sequential SISO design strategy achieves the smallest average variance of the single-stage VCM tracking error. Moreover, the VCM activity in terms of the control input as shown in Fig. 9 is largest for the sequential SISO design strategy amongst all the

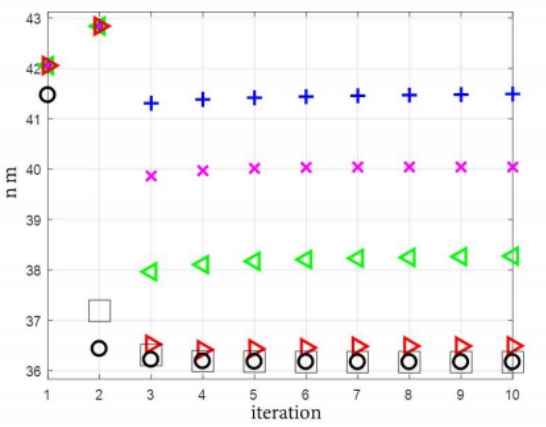

FIGURE 8. The H_2 objective $\sqrt{\frac{1}{l}\sum_{i=1}^{l}||e_i^s||_2}$ used for the optimization problem is plotted versus the iteration number. The square shows the upper bound used for the optimization problem. The other markers represent real values as per Table 1.

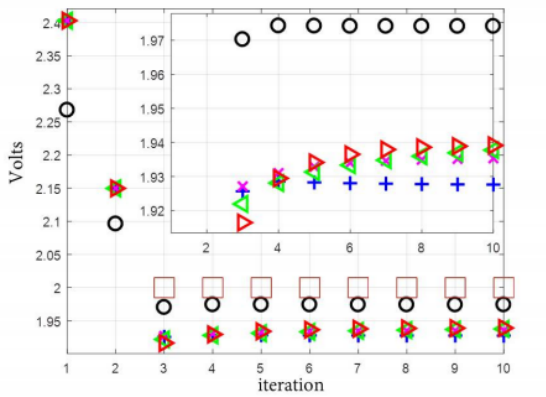

FIGURE 9. H_2 norm constraint: $\sqrt{\frac{1}{l}\sum_{i=1}^{l}||u_{vi}^s||_2}$. The square shows the upper bound used for the optimization problem. The other markers represent real values as per Table 1.

five scenarios.

Considering the SIMO design strategy, the MA output stroke is restricted in the design process as given in Eq. (24). As the restriction on the MA stroke becomes more severe, the ability of the MA to reduce the tracking error decreases. The sensitivity decoupling structure dictates that VCM should compensate for the MA, and this can be observed as an increase in the VCM activity shown Fig. 9. This is reflected in a smaller average variance single-stage VCM tracking error for larger VCM control input activity, as shown in Fig. 8.

Fig. 10 shows that the weighted H_∞ norm constraint on the closed loop transfer function $E_{r\to e}^s$ in Eq. (18) was met for all the five scenarios. There are five plots, each corresponding to five

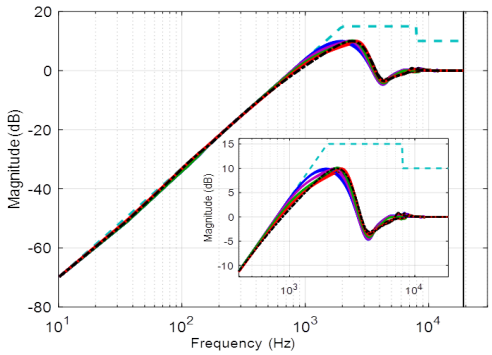

FIGURE 10. Magnitude Bode Plots of H_∞ constraints on the closed loop transfer function $E_{r\to e}^s$ for all the five frequency response measurements for each scenario. The dotted line shown is the weighting function used in the design process. It can be observed that the H_∞ constraints are met for all the frequency response measurements.

frequency response measurements used for each scenario from Table 1.

Sequential SISO Strategy vs SIMO strategy

If the SIMO Design strategy is successful to find a feasible solution for the optimization problem there is no guarantee that the sequential SISO design problem will also be able to find a feasible solution for its corresponding optimization problem. To exemplify this, a weighting function for the H_∞ norm condition on the closed loop transfer function $U_{w_v\to u_m}$ in Eq. (19) was adjusted to place more restriction at higher frequencies. Fig. 11 shows that both sequential SISO design strategy and the SIMO design strategy succeed in finding a feasible solution for the lenient *blue* weighting function. Whereas, only the SIMO strategy gave a feasible solution for the stricter *red* weighting function.

The order of the SIMO controller $\bar{K}$ used to obtain the results presented was 25. The compensators K_v and K_m were obtained using Eq. (25). The order of these compensators K_v and K_m can be reduced upto 17 and 20 respectively. These same orders were used in the sequential SISO design strategy.

CONCLUSION

A frequency domain data driven mixed H_2/H_∞ control synthezis algorithm was studied and applied to a dual-stage HDDs. The data driven algorithm directly uses the frequency response measurements of several plants, hence accounting for plant variations in the product line and variations among multiple MA's in multiple platter drives. The stability of the closed loop system and a specified performance levels can be achieved by the algorithm if enough number of frequency response data measurements are used to represent the dynamic uncertainties and resonant modes variations of the actual plants.

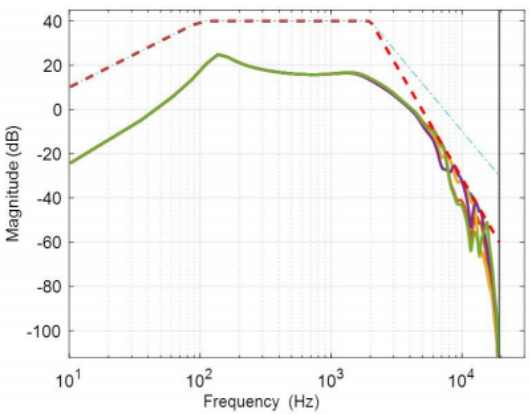

FIGURE 11. H_∞ constraint on the closed loop transfer function $U_{w_v \to u_m}$ is shown. Two weighting functions are considered: loose constraint (light blue dotted line) and the strict constraint (red dotted line). The SIMO design strategy was able to meet both constraints, as shown by the solid plots in the figure (each plot represents a different plant), but the sequential SISO design strategy was unable to find a feasible controller that could meet the stricter constraint.

The data driven control design method simultaneously addresses average H_2 performance and constraints and objectives robust control objectives and H_∞ robustness objectives for multiple plant frequency responses. The H_infty and H_2 norm constraints were simultaneously solved in an iterative manner as a locally convex constrained optimization problem. The data driven control design methodology was used to design track following controllers for dual-stage HDDs. The controller was chosen to have a sensitivity decoupling structure. Two strategies were implemented to obtain the controller in this structure: Sequential SISO design strategy and SIMO design strategy.

The dual stage controller was designed using a set of five frequency response measurement data for both of the actuators. The design results showed that the data driven design approach successfully met the mixed H_2/H_∞ design objectives. As expected the SIMO design strategy, which simultaneously optimizes the controllers for both the VCM and the MA, achieves a smaller average variance in the tracking error and performs better than the sequential SISO design strategy.

REFERENCES

[1] Kasavajhala, V., 2011. "Sold state drive vs. hard disk drive price and performance study". *Proc. Dell Tech. White Paper*.

[2] Yi, L., and Tomizuka, M., 1999. "Two-degree-of-freedom control with robust feedback control for hard disk servo systems". *IEEE/ ASME transactions on mechatronics,* ***4***(1), pp. 17–24.

[3] Mori, K., Munemoto, T., Otsuki, H., Yamaguchi, Y., and Akagi, K., 1991. "A dual-stage magnetic disk drive actuator using a piezoelectric device for a high track density". *IEEE Trans. Magnetics,* ***27***, Nov., pp. 5298–5300.

[4] Li, Y., and Horowitz, R., 2001. "Mechatronics of electrostatic microactuators for computer disk drive dual-stage servo systems". *IEEE/ASME Trans. Mechatronics,* ***6***(2), pp. 111–121.

[5] Kobayashi, M., and Horowitz, R., 2001. "Track seek control for hard disk dual-stage servo systems". *IEEE Transactions on Magnetics,* ***37***(2), pp. 949–954.

[6] Horowitz, R., Li, Y., Oldham, K., Kon, S., and Huang, X., 2007. "Dual-stage servo systems and vibration compensation in computer hard disk drives". *Control Engineering Practice,* ***15***(3), pp. 291–305.

[7] Abramovitch, D., and Franklin, G., 2002. "A brief history of disk drive control". *IEEE Control Systems,* ***22***(3), pp. 28–42.

[8] Hernandez, D., Park, S., Horowitz, R., and Packard, A., 1999. "Dual-stage track-following servo design for hard disk drives". In American Control Conference, Vol. 6 of *Proceedings of 1999*, IEEE, pp. 4116–4121.

[9] Galdos, G., Karimi, A., and Longchamp, R., 2010. "H-infinity controller design for spectral mimo models by convex optimization". *Journal of Process Control,* ***20***(10), pp. 1175–1182.

[10] Karimi, A., and Kammer, C. "A data driven approach to robust control of multivariable systems by convex optimization". *Automatica*.

[11] Karimi, A., Nicoletti, A., and Zhu, Y., 2016. "Robust h-infinity controller design using frequency domain data via convex optimization". *International Journal of Robust and Non Linear Control*.

[12] Bazanella, A. S., Campestrini, L., and Eckhard, D., 2011. "Data-driven controller design: the h2 approach". *Springer Science and Business Media*.

[13] Bagherieh, O., 2017. "Estimation, identification and data-driven control design for hard disk drives". PhD thesis, University of California, Berkeley. https://escholarship.org/uc/item/0998n097.

[14] Khargonekar, P. P., and Rotea, M. A., 1991. "Mixed h2/h-infinity control: a convex optimization approach". *IEEE Transactions on Automatic Control,* ***36***(7), pp. 824–837.

[15] Tay, T. T., Moore, J. B., and Horowitz, R., 1989. "Indirect adaptive techniques for fixed controller performance enhancement". *International Journal of Control,* ***50***(5), pp. 1941–1959.

[16] Lofberg, J., 2004. "Yalmip: A toolbox for modeling and optimization in matlab". In Computer Aided Control Systems Design, 2004, IEEE International Symposium on, IEEE, pp. 284–289.